Effect of Hydrophobicity on the Interaction between Antimicrobial Peptides and Poly(acrylic acid) Microgels

Helena Bysell,*,† Per Hansson,† Artur Schmidtchen,‡ and Martin Malmsten†

Department of Pharmacy, Uppsala University, P.O. Box 580, SE-751 23 Uppsala, Sweden, Section of Dermatology and Venereology, Department of Clinical Sciences, Lund University, SE-221 84 Lund, Sweden

Received: October 21, 2009; Revised Manuscript Received: November 25, 2009

The influence of peptide hydrophobicity on the interaction between antimicrobial peptides and poly(acrylic acid) microgels was studied by end-tagging the kininogen-derived antimicrobial peptide GKHKNKGKKNGKHNGWK (GKH17) and its truncated variant KNKGKKNGKH (KNK10) with oligotryptophan groups of different lengths. Microgel deswelling and reswelling in response to peptide binding and release was studied by micromanipulator-assisted light- and fluorescence microscopy, peptide uptake in microgels was determined from solution depletion measurements, and peptide oligomerization was monitored by fluorescence spectroscopy. Results showed that oligomerization/aggregation of the hydrophobically end-tagged peptides is either absent or characterized by exposure of the tryptophan residues to the aqueous ambient, the latter suggesting small aggregation numbers. In addition, peptide uptake and affinity to the poly(acrylic acid) microgels increase with the number of trypthophan residues in the hydrophobic end tag, whereas peptide-induced microgel deswelling kinetics did not display this tag-length dependence to the same extent. Instead, long end tags resulted in anomalous shell formation, opposing further peptide-induced network deswelling. Theoretical modeling suggested that the deswelling kinetics in response to peptide binding is largely controlled by stagnant layer diffusion, but also that for peptides with sufficiently long hydrophobic tags, the shell constitutes an additional diffusion barrier, thus resulting in slower microgel deswelling. In addition, GKH17 and KNK10 peptides lacking the tryptophan end tags were substantially released on reducing peptide−microgel electrostatic interactions through addition of salt, an effect more pronounced for the shorter KNK10 peptide, whereas the hydrophobically end-tagged peptides remained bound to the microgels also at high ionic strength.

Introduction

Microgels are materials that can be designed to fit a range of interesting applications; for example, as biomaterials or functional and protective carriers for protein and peptide drugs.[1−5] For instance, it has been reported that proteins entrapped in microgels can be released in response to some external stimuli inducing microgel swelling.[6,7] Despite this, only a few studies have, to our knowledge, been reported so far concerning the details of the interactions involved in microgel−peptide/protein systems. Considering this, we previously performed a series of investigations addressing this issue,[8−13] mainly focusing on the effects of electrostatics and peptide length on peptide/protein incorporation into, distribution within, and release from, charged and weakly cross-linked microgels. For instance, the possibility to control the binding and release of repeat sequence peptides to and from microgels by electrostatics, such as changes in pH or ionic strength, was recently evaluated.[11]

One interesting group of peptides that potentially would benefit from inclusion in anionic microgels is antimicrobial peptides (AMPs).[14] These peptides are small (∼10−40 amino acid residues) and cationic and constitute an important part of our innate immune system.[15] Although the mechanism by which AMPs kill bacteria is complex, including DNA binding and protein synthesis interference,[16,17] and also varies between peptides, one of its central features involves electrostatic interactions between these cationic peptides and anionic components of bacterial cell walls, resulting in disruption of the latter.[18−21] Through this, AMPs display potent, fast, and broad-spectrum bactericidal activity at seemingly limited bacterial resistance development.[14,16,22] By using approaches such as structure−activity relationship in combination with single amino acid variations,[23,24] as well as identification of antimicrobial peptides from endogenous origin,[25−29] good selectivity between bacteria and eukaryotic cells can be obtained for such peptides, which thus have potential as novel antibiotics. To reach their full potential, delivery systems may offer opportunities for efficient and safe AMP delivery,[30−32] for example, related to protection from chemical and proteolytic degradation;[29,33] problematic (e.g., in wound infections[22,34]), sustained or triggerable release; reduced toxicity; and increased bioavailability. To enable such potential AMP delivery systems based on polyelectrolyte microgels, detailed investigations on AMP−microgel interactions are needed. Given the action mechanisms of AMPs outlined above, studies on the interactions between AMPs and anionic microgels may also be relevant for understanding the mechanism of action of such peptides better, particularly regarding AMP binding to polysaccharide components in the bacterial walls.

The peptides GKHKNKGKKNGKHNGWK (GKH17) and its truncated variant KNKGKKNGKH (KNK10) (Table 1) are derived from human kininogen and have an antimicrobial effect toward both Gram-positive and Gram-negative bacteria.[26] However, at physiological salt concentration, this activity is largely reduced. To overcome this, these and other kininogen-based AMPs have been end-tagged with hydrophobic oligopep-

* Corresponding author. E-mail: helena.bysell@farmaci.uu.se.
† Uppsala University.
‡ Lund University.

10.1021/jp910068t
Published on Web 01/04/2010

TABLE 1: Properties of the Peptides Studied

peptide name	peptide sequence	net charge pH 7.4	M_w (g/mol)	hydropathy index[a]
KNK10	KNKGKKNGKH	+5	1138	−3.05
KNK10W3	KNKGKKNGKHWWW	+5	1697	−2.55
KNK10W5	KNKGKKNGKHWWWWW	+5	2069	−2.33
GKH17	GKHKNKGKKNGKHNGWK	+7	1946	−2.75
GKH17W3	GKHKNKGKKNGKHNGWKWWW	+7	2507	−2.47
GKH17W6	GKHKNKGKKNGKHNGWKWWWWWW	+7	3064	−2.27

[a] The average hydropathy (hydrophobicity) index of aminoacids in the peptide sequences as calculated from the Kyte and Dolittle scale.[56]

tide stretches, which dramatically increases their antimicrobial potency for a range of Gram-positive and Gram-negative bacteria,[35,36] not negatively affecting the proteolytic stability of the template peptides, as well as retaining low cytotoxicity, properties interesting from a therapeutic perspective.

In addition to offering therapeutic potential, such end-tagged peptides are interesting also for model studies of the role of peptide hydrophobicity; for example, in peptide interaction with microgels, since peptide hydrophobicity can be changed in a sequence-independent manner, not affecting the random coil structure formed by these peptides.[36] In the present study, a few such end-tagged peptides were therefore chosen as model peptides for investigating the effect of peptide hydrophobicity on peptide interaction with oppositely charged microgels. Peptide−microgel interactions were investigated with micromanipulator-assisted light and fluorescence microscopy, focusing on the microgel deswelling and reswelling in response to peptide binding and release, with fluorescence spectroscopy for probing possible peptide self-assembly in the microgels, and with solution depletion measurements to estimate the peptide uptake in the microgels. In addition, the kinetics of peptide-induced microgel deswelling kinetics was analyzed theoretically.

Experimental Section

Materials. *N*,*N*′-methylenebisacrylamide, and *N*,*N*,*N*′,*N*′-tetramethyl-ethylenediamine (TEMED), ammonium persulfate, and acrylic acid were from Sigma-Aldrich (Steinheim, Germany), and sorbitan monostearate (Span 60) was from Carl Roth (Karlsruhe, Germany). The peptides (GKH17, GKH17W3, GKH17W6, KNK10, KNK10W3, and KNK10W5; Table 1) were all synthesized by Biopeptide Co. (San Diego, CA). The purity of the peptides was confirmed to be >95% by MALDI-TOFMS analysis (Voyager, Applied Biosystems). For pH control, 10 mM Tris buffer at pH 7.4 was used. All other chemicals were of analytical grade. Purified Milli-Q water was used throughout.

Preparation and Characterization of Microgels. Poly(acrylic acid) microgel particles were synthesized by inverse suspension polymerization, as described previously.[9] In brief, 0.05 g of Span 60 was dissolved in 20 mL of cyclohexane, and the resulting solution was preheated to 45 °C and stirred at 1000 rpm under nitrogen atmosphere. A mixture of 2.6 g of acrylic acid, 0.1 g of *N*,*N*′-methylenebisacrylamide, 20 g of NaOH (2 M), 4 g of NaCl, and 60 μL of TEMED was then prepared. Ten milliliters of this reaction mixture was mixed with 0.5 mL of 0.18 M ammonium persulfate solution and added to the preheated cyclohexane solution. The polymerization was performed at 65 °C under nitrogen atmosphere to prevent quenching by oxygen. The reaction proceeded for 30 min, followed by addition of 40 mL of methanol. Gel particles were then left to sediment overnight and then washed repeatedly with methanol and water. Gel particles were sieved using a Retsch 5657 test sieve (Haan, Germany). Fractions below the mesh size of 300 μm were collected and stored in water. The dry mass of these microgels was determined from freeze-drying experiments to be 1.7 mg gel/g gel solution using a Flexidry μP freeze-dryer (Kinetics Thermal Systems, Stone Ridge, NY). The charge content of the microgels was estimated from base titration. In brief, 20 g of microgel suspension was pH-adjusted to pH 1.8 by addition of HCl (1 M). NaOH (0.1 M) was then added from a buret, and the pH was monitored using a Metrohm 654 pH-meter (Switzerland). From the titration curve (Figure S1 of the Supporting Information), the charge content in the microgels could be calculated to 3.3 ± 0.2 μmol/mg of dry gel. The swelling/deswelling of the microgels was totally reversible when changing pH or ionic strength, and reversibility persisted beyond one swelling/deswelling cycle.

Effects of Peptide Binding and Release Monitored by Microscopy. Changes in microgel volume upon peptide binding and release were monitored, in at least triplicate measurements, by micromanipulator-assisted microscopy using an Olympus Bx-51 light microscope (Olympus, Tokyo, Japan) equipped with an ONM-1 manipulator (Narishige, Tokyo, Japan) and a DP 50 digital camera (Olympus, Tokyo, Japan). Micropipets (10−20 μm in diameter) were prepared with a PC-10 puller and a MF-9 forger (both Narishige, Tokyo, Japan). Gel particles were captured by micropipet suction using an IM-5A injector (Narishige, Tokyo, Japan) placed inside a 2-mm-diameter flow pipet and flushed with peptide solution using a peristaltic pump P-1 (Pharmacia, Uppsala, Sweden) at a flow rate of 1.8 mL/min. (Although micropipet suction may affect microgel shape, its effect on microgel volume is of minor importance.) This experimental setup allows the peptide concentration outside the microgel particle to be unaffected by peptide uptake in the gels. Microgels were photographed every 30 s using Viewfinder, Studio 3.0.1 (Pixera, San Jose, CA), and the gel particle diameter was measured using Olympus DP-soft software (Olympus, Tokyo, Japan). The volume ratio is expressed as V/V_0, were V is the volume of a gel particle after exposure to peptide for a certain time, and V_0 is the volume of the gel particle at pH 7.4 and 10 mM ionic strength. The peptide-induced volume response of single poly(acrylic acid) microgels (∼100 μm in diameter when fully swollen) upon binding of antimicrobial peptides (5 μM) was studied at pH 7.4 and 10 mM ionic strength by peptide flushing for 20 min. To investigate electrolyte-induced release of peptides, microgels were flushed with pH 7.4 buffer solution of ionic strength 150 and 220 mM for 20 min after peptide binding, followed by buffer replacement to 10 mM ionic strength, to be able to compare the final gel volume, because this itself is influenced by the ionic strength. The results are presented as the average and standard deviation of deswelling ratios obtained from at least three single microgel experiments. In addition, the peptide distribution during and after microgel deswelling was analyzed with fluorescence microscopy using the same microscopy setup, but with an Olympus U-RFL-T UV-lamp (Olympus, Tokyo, Japan), for monitoring the autofluo-

rescence of tryptophan residues in the peptides (thus requiring no fluorescence labeling).

Uptake of Peptides in Microgels. Peptide uptake in microgels was measured using a depletion method, as previously described.[9,10] In brief, 250 μL of peptide solution (in the concentration range 10−500 μM at pH 7.4 and ionic strength 10 mM) was mixed with 50 μL of microgel suspension and allowed to equilibrate for at least 48 h. The microgel−peptide complexes thus formed were then separated by centrifugation at 4000 rpm for 10 min. At this centrifugation time and speed, the influence of active peptide transport out of the microgels due to microgel compression was presumed to be negligible. The amount of peptides remaining in solution was determined by Bicinchonic acid assay[37] using a Saphire plate reader (Tecan, Männedorf, Switzerland) at $\lambda = 562$ nm and compared to the peptide concentration in a solution without gels. The amount of microgel-bound peptide charges ($R_{complex}$ = mole positive peptide charges/mol negative microgel charges) at various initial charge ratios ($R_{initial}$ = mole positive peptide charges/mol negative microgel charges) was determined.

Peptide Oligomerization Monitored by Fluorescence Spectroscopy. Tryptophan fluorescence was measured using a Saphire plate reader (Tecan, Männedorf, Switzerland), using an excitation wavelength of 280 nm and recording emission spectra between 310 and 450 nm. Measurements were conducted on peptides in solution and when bound to microgels. To maximixe the signal from microgel-bound peptides and minimize the contribution from unbound peptide, tryptophan fluorescence was monitored at conditions of high peptide uptake and low free peptide equilibrium concentration, on the basis of peptide uptake results. All measurements were performed at pH 7.4 and 10 mM ionic strength.

Theoretical analysis

Theoretical Model. The analysis of the change of volume of a single gel microgel bead in contact with a peptide solution is subject to the following conditions: (1) The gel is pre-equilibrated with the liquid at zero peptide concentration. (2) The volume change on peptide addition is the result of a core-to-shell phase transition, where the peptide−microgel complex phase formed in the surface region represents the shell and the peptide-free, swollen microgel network represents the core. (3) The rate of the phase transition reaction is controlled by the steady-state transport of peptide to the core/shell boundary, where the shell (surface phase) grows at the expense of the swollen gel core. (4) Local equilibrium is maintained at the shell/core (r_1) and shell/liquid (r_2) boundaries. (5) At the onset of shell formation, the chemical potential of all components is the same in the shell, core and liquid. The resulting concentration of peptide ion and network chains in the shell is assumed to be unchanged during shell growth, as is the chemical potential of the peptide salt PX_m (see below) at the core/shell boundary. (6) Simple salt (MX) is in excess over the peptide salt everywhere in the liquid.

The system contains four components: water and three electrolytes. The electrolytes can be chosen arbitrarily as PX_m, MX, and PN_m, where P is a peptide ion, M is a monovalent cation, X is a monovalent anion, N is part of a network chain containing one negative charge, and m is the number of anions forming a salt together with a peptide ion. It is consistent with the above conditions that the chemical potentials of water, MX, and PN_m remain essentially uniform in the shell. A peptide is transported through the shell when the chemical potential of PX_m is larger at r_2 than at r_1. The chemical potential of PX_m in the liquid at r_2 can be written as

$$\mu_{PX_m}^{liq} = \mu_P^{0,w} + RT \ln \gamma_P C_P + m\mu_X^{0,w} + mRT \ln \gamma_X C_X \quad (1)$$

where $\mu_i^{0,w}$ denotes the standard contribution (infinite dilution in water); γ_i, the activity coefficient; and C_i, the concentration of i. Let C_2 be the peptide concentration in the liquid at r_2 and C_2^*, the corresponding concentration required for onset of shell formation. In a dilute peptide solution with salt present in excess where γ_P, γ_X, and C_X are independent of C_P, the difference in chemical potential over the shell is

$$\Delta\mu = \mu_{PX_m}(r_2) - \mu_{PX_m}(r_1) = RT \ln \frac{C_2}{C_2^*} \quad (2)$$

The radial flux at a distance r from the gel center is given by the generalized form of Fick's first law:

$$\frac{dn}{dt} = -\frac{4\pi r^2 DC}{RT} \frac{d\mu}{dr} \quad (3)$$

where D is the diffusion constant, R is the gas constant, and T is the absolute temperature. At constant peptide concentration in the shell C_{shell} one obtains from eq 3 the steady-state flux through the shell.[51]

$$\frac{dn_P}{dt} = \frac{4\pi r_1 r_2 D_{shell} C_{shell} \Delta\mu}{(r_2 - r_1)RT} = \frac{4\pi r_1 r_2 D_{shell} C_{shell} \ln(C_2/C_2^*)}{(r_2 - r_1)} \quad (4)$$

Since all processes, except peptide transport, relax on short time scales, the gel dimensions (r_1, r_2) can be considered functions of the number of moles of peptide transported, n_P, only.[47,51] It follows that eq 4 can be integrated to give the time it takes for n_P peptides to bind. The result is

$$t = \frac{R_0^3}{3v_0 Z D_{shell} C_{shell}} \int_0^\beta \frac{r_1^{-1} - r_2^{-1}}{\ln(C_2/C_2^*)} d\beta \quad (5)$$

where β is the total peptide-to-network charge ratio in the gel

$$\beta = \frac{3v_0 Z n_P}{4\pi R_0^3} \quad (6)$$

Z is the peptide charge, R_0 is the gel radius, and v_0 is the volume per network charge in the gel, respectively, prior to binding. The integral in eq 5 can be calculated using the relationships[51]

$$\left(\frac{r_2}{R_0}\right)^3 = f\beta v_{shell}/v_0 + (1 - f\beta)v_{core}/v_0 \quad (7)$$

$$\left(\frac{r_1}{R_0}\right)^3 = (1 - f\beta)v_{core}/v_0 \quad (8)$$

where v_{shell} is the volume per network charge in the shell, and v_{core} is the corresponding quantity in the core, and f is the polyion-to-peptide charge ratio in the shell, so that $f\beta$ is the fraction of the network chains located in the shell and $C_{shell} = (Zfv_{shell})^{-1}$. C_2 depends on the rate of mass transfer from the bulk liquid to the gel surface, conveniently calculated from the peptide diffusion constant in water (D_{liq}) and the Sherwood number (Sh):[47,51,52]

$$\frac{dn_P}{dt} = 4\pi r_2(1 + Sh/2)D_{liq}(C_{bulk} - C_2) \quad (9)$$

$$Sh = 2.0 + 0.6(Re)^{1/2}(Sc)^{1/3} \quad (10)$$

$$Re = \frac{2vr_2\rho}{\eta} \quad (11)$$

$$Sc = \frac{\eta}{\rho D_{liq}} \quad (12)$$

where v is the liquid flow rate, ρ is the liquid density, and η is the liquid viscosity. At steady state, the flux is the same in eqs 4 and 9, giving

$$C_2 = C_{bulk} - \frac{r_1 D_{shell} C_{shell} \ln(C_2/C_2^*)}{(r_2 - r_1)(1 + Sh/2)D_{liq}} \quad (13)$$

to be solved iteratively for C_2.

When the net transport is controlled by mass transfer to the gel surface ("stagnant layer control"), eqs 5 and 13 can be replaced by

$$t = \frac{R_0^3}{3v_0 Z D_{liq}(C_{bulk} - C_2^*)} \int_0^\beta \frac{1}{r_2(1 + Sh/2)}\, d\beta \quad (14)$$

With the present notations, the composition of the shell is determined by f and v_{shell}. The former is available from binding isotherms, and the latter is taken to be the same as in the fully collapsed state when the core has vanished and the gel volume is V_{min}; that is, the model uses experimentally based input. This is consistent with the description of the deswelling as a phase transition. Thus,

$$\frac{v_{shell}}{v_0} = \frac{V_{min}}{V_0} \quad (15)$$

In the absence of elastic effects, the compositions of the coexisting phases should be fixed during the phase transition. Investigations of related systems show that, although this may be a good approximation for the shell, the volume per network charge in the core (v_{core}) can decrease with increasing fraction of network in the shell ($f\beta$).[53,54] This has been attributed to an additional contribution to the osmotic pressure in the core due to the work of elastic deformation of the shell network. A description of the effect can be incorporated in the kinetic framework, as demonstrated elsewhere.[47,49,51,55] However, to simplify the calculations, we use an approximate expression,

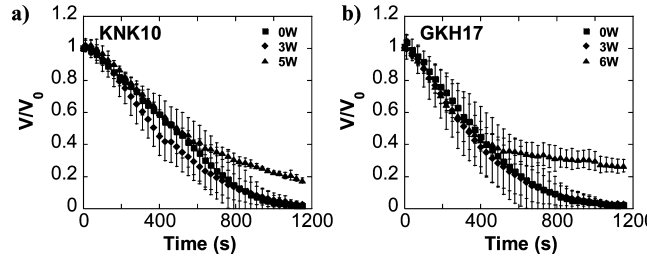

Figure 1. Experimental microgel deswelling curves after addition of (a) KNK10 and (b) GKH17 peptides (5 μM) with an increasing number of hydrophobic tags, W, at pH 7.4 and 10 mM ionic strength.

$$\frac{v_{core}}{v_0} = (1 - f\beta)^\alpha \quad (16)$$

With $\alpha = 1$, eq 16 has been found to capture the effect quite well at equilibrium.[47,54] In a dynamic situation, the effect may be absent ($\alpha = 0$) or partly developed ($0 < \alpha < 1$) if the relaxation of the shell network is sufficiently slow.

In the calculations, we used $R_0 = 50$ μm, in agreement with the experimentally observed gel sizes, whereas $v_0 = 0.026$ m^3/mol was determined earlier at 10 mM salt for the present microgels,[51] and $D_{liq} = 1.6 \times 10^{-10}$ m^2/s was determined for GKH17 with dynamic light scattering.[36] f was set to 1.2, 0.83, and 0.71, for GKH17, GKH17W3, and GKH17W6, respectively, corresponding to the maximum experimental binding ratios obtained in the peptide uptake measurements (Figure 5b below), and v_{shell} was set to 5.2×10^{-4} and 7.8×10^{-4} m^3/mol GKH17 and GKH17W3, respectively, as calculated from the final gel volume according to eq 15. For GKH17W6, such a calculation was not possible, since the gel did not reach the fully collapsed state (see below). In all curves, a small (30−55 s) lag time was used as a fitting parameter added to correct for the fact that deswelling does not start at time zero. This time can be interpreted as the time required for formation of a concentration gradient in the stagnant layer in the liquid and is similar to the lag times obtained in previous investigations.[49,51]

Results and Discussion

End-tagging antimicrobial peptides KNK10 and GKH17 with short oligotryptophan stretches does not influence the peptide-induced microgel deswelling kinetics to any significance, as seen when comparing untagged and 3W-tagged peptides (Figure 1). Since electrostatic interaction is the major driving force for peptide binding and microgel deswelling in this system,[10] and because peptide charge is unaffected by the tryptophan end-tagging, this result is not surprising. Strikingly, however, when increasing the number of tryphtophan residues further (to GKH17W6 and KNK10W5, respectively), peptide-induced microgel deswelling ceases earlier (already at ~600 s) than for the nontagged peptides, resulting in a decreased microgel deswelling response (i.e., final deswelling ratios) of ~0.2−0.3 as compared to ~0.02−0.03 for GKH17W6 and GKH17, respectively. Similar results were obtained for KNK10W5 (Figure 1). In analogy to previous findings,[8−10] the decreased deswelling response obtained for KNK10W5 and GKH17W6 may be interpreted as originating from strong peptide−gel complex formation. This results in the formation of a dense surface shell (Figure 2b, c) for KNK10W5 and GKH17W6, but

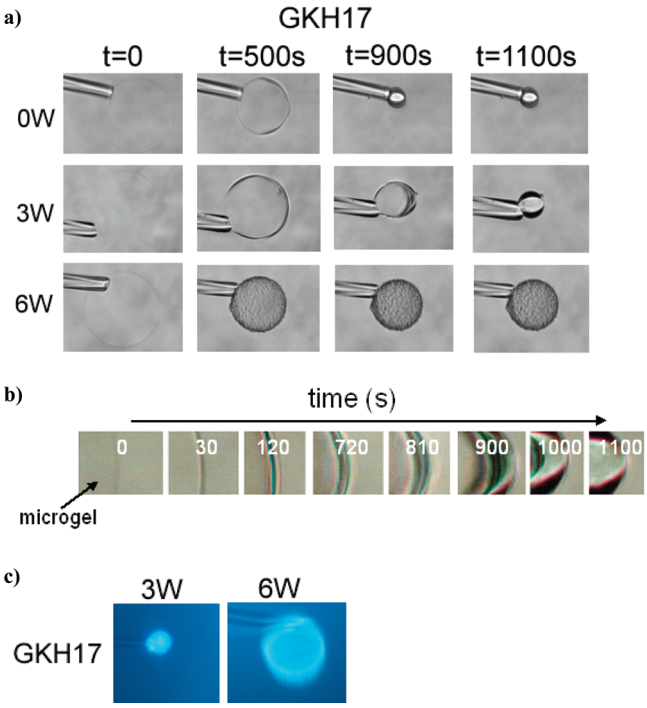

Figure 2. (a) Exemplifying microscopy images showing the influence of tryptophan end-tagging on the deswelling of microgels upon addition of 5 μM GKH17 peptides at pH 7.4 and ionic strength 10 mM. (b) Enlarged images showing the formation of a dense peptide−gel skin layer at various times after addition of 5 μM GKH17W3. (c) Fluorescence microscopy images, displaying the final peptide distribution (at $t = 1100$ s) of tagged peptides in microgels.

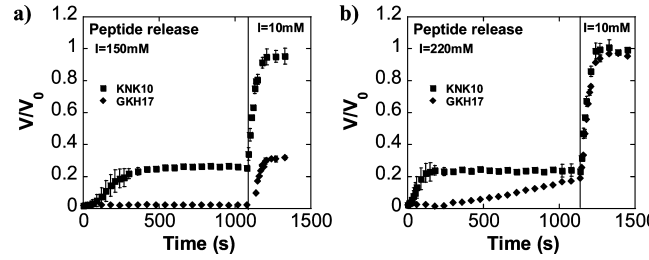

Figure 3. Electrolyte-induced microgel reswelling kinetics, mirroring peptide release kinetics, obtained with untagged peptides at pH 7.4 and (a) 150 mM or (b) 220 mM ionic strength. Note that after the electrolyte-induced release step, the ionic strength was turned back to 10 mM again, to be able to compare the volume ratio, and thereby estimate the amount of peptide released.

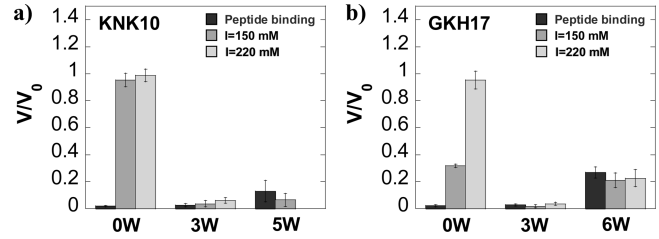

Figure 4. Volume ratio, V/V_0, of microgels after peptide binding at pH 7.4 and ionic strength 10 mM, and after electrolyte-induced release at pH 7.4 and an ionic strength of either 150 or 220 mM for (a) KNK10 and (b) GKH17 peptides with different lengths of the hydrophobic tag.

not for the peptides with shorter end tags. The shell hinders further diffusion of peptides into microgels and provides a mechanical opposition to further peptide-induced network deswelling, thereby displaying a confined distribution of peptides within the microgel surface layer (Figure 2c). These results are in analogy with a recent investigation on drug molecules interacting with functionalized p(NIPAM) microgels, in which a more condensed skin layer was formed for more hydrophobic drugs.[38]

Although an increased peptide size was previously shown to enhance the peptide-induced microgel deswelling kinetics,[11] no distinction could be made between GKH17 and its truncated variant KNK10 in the present study. However, in the present case, the shorter KNK10 peptide has a higher degree of charge than the longer GKH17 (50 vs 41 mol % of the amino acids charged). The higher charge density of KNK10 thus compensates for its smaller size because a higher peptide charge density also leads to a larger deswelling response.[10,11] The microgel deswelling induced by KNK10 is analogous to previously reported results on the heparin-binding consensus peptide AKKARAAKKARA, in the same size range and with the same overall peptide charge degree.[11] Although the hydrophobic/hydrophilic scaling of amino acids residues is complex and strongly varies between different scaling methods,[39−41] this previous peptide can be considered more hydrophobic (−1.15 on Kyte and Doolittle scale) than the presently investigated peptides (−2.27 to −3.05; Table 1), again emphasizing the importance of electrostatic interactions in these systems, at least when it comes to peptide-induced microgel deswelling.

Peptides incorporated into microgels by electrostatic attraction can be released by decreasing the strength of the interactions involved, for example, by changing the pH to decrease the charge density of the peptide or microgel (or both) or by increasing the ionic strength in the surrounding medium.[11] In the present study, the untagged peptide KNK10 was completely detached within ∼7 min in 150 mM ionic strength and even faster (within ∼3 min) in 220 mM ionic strength (within ∼3 min), whereas the longer untagged GKH17 was only partially released at 150 mM and completely released first after ∼20 min in 220 mM ionic strength (Figure 3). These results, which are analogous to previous findings obtained for $(AKKARA)_n$ and $(ARKKAAKA)_n$ consensus peptides of varying length,[11] are expected, since the probability of simultaneous detachment of all peptide segments from the oppositely charged network decreases strongly with the peptide length. Increasing the peptide hydrophobicity through end-tagging by oligotryptophan stretches, however, totally eliminated peptide detachment from the microgel network with increased ionic strength (Figure 4). Because high electrolyte concentrations reduce electrostatic interactions, whereas hydrophobic interactions are largely unaffected by ionic strength, these results demonstrate the increased contribution of hydrophobic interactions for end-tagged peptides bound to microgels. An analogous increased electrolyte resistance in binding to oppositely charged polyelectrolytes was previously observed for both GKH17W3 and KNK10W5 binding to bacterial lipopolysaccharide at high ionic strength.[35,36] In addition, end-tagging KNK10 and GKH17 peptides with tryptophan residues (>4 W) drastically increased the membrane disruptive and bactericidal properties at physiological salt concentrations,[35,36] demonstrating the importance of hydrophobic interactions also for the mechanism of action of these peptides.

Although effects of tryptophan end-tags were modest in terms of peptide-induced deswelling, oligotrypthophan end-tagging expectedly resulted in larger peptide uptake and steeper binding isotherm at charge ratios <1 for tagged peptides, in comparison to the untagged ones (Figure 5), emphasizing the presence of hydrophobic interactions in addition to electrostatic ones. Although electrostatic interactions are expected to be dominant in highly charged microgel−peptide systems, such as the

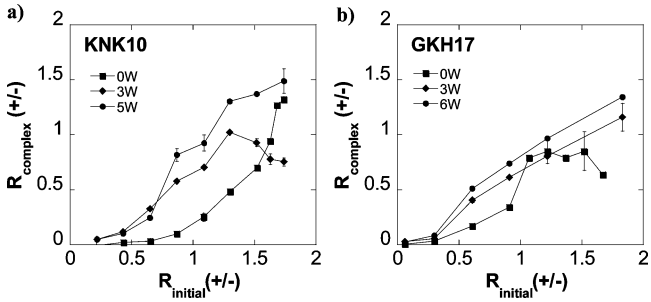

Figure 5. Influence of tryptophan end-tagging on the uptake (charge ratio) of peptides in microgels as a function of initial charge ratio for (a) KNK 10 and (b) GKH17 at pH 7.4 and ionic strength 10 mM.

TABLE 2: Tryptophan Emission Maxima Obtained for Tryptophan-Tagged Peptides in Solution and When Incorporated into Microgels

peptide	λ_{max} (nm) in solution	λ_{max} (nm) in microgels
KNK10W3	368	369
KNK10W5	370	370
GKH17W3	370	365
GKH17W6	361	363

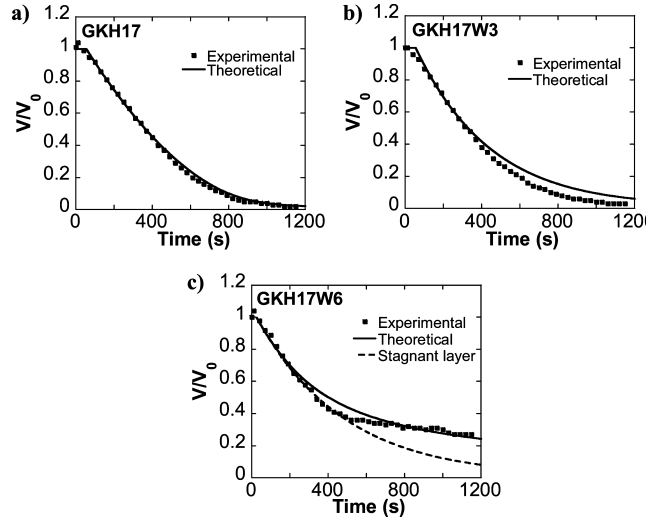

Figure 6. Theoretical deswelling curves (solid line) describing the deswelling of microgels upon addition of (a) untagged GKH17 and (b) GKH17 end-tagged with 3 and (c) 6 tryptophan residues. For comparison, experimental results are included as solid squares. In panel c, the dashed line displays the theoretical analysis corresponding to pure, stagnant-layer-diffusion-controlled kinetics.

presently investigated ones, hydrophobic interactions could nevertheless play a significant role, especially for peptides (or microgels, or both) with well-defined hydrophobic domains (such as the presently investigated with end-tagged peptides) or with high overall hydrophobicity. In fact, hydrophobic interactions have been shown to dominate over electrostatic interactions in complex formation of cationic surfactants with both linear[42−44] and cross-linked[45,46] poly(acrylic acid) at low degrees of neutralization or hydrophobic modification of the latter. Because the concentration of free dissociated carboxylic acid residues is dramatically reduced upon binding of oppositely charged peptides and polymer chains in the network adopt a less extended conformation, the significance of hydrophobic interactions is likely to increase in later stages of microgel deswelling. This could then contribute to the strong interaction between tagged peptides and microgels displayed in the present investigation, particularly at high ionic strengths. In comparison, the insignificant release of hydrophobic drug molecules from functionalized p(NIPAM) microgels at high ionic strength also demonstrates the importance of hydrophobic interactions.[38]

To some extent, the peptide-induced deswelling response for these peptides (Figure 1), with the appearance of a dense peptide−microgel skin layer during the volume transition time (Figure 2), resembles that resulting from cationic surfactant binding to poly(acrylic acid) microgels.[45−49] As in the presently investigated peptide systems, the major driving force for the interaction between cationic surfactant micelles and anionic microgels is electrostatic attraction. However, because surfactant binding is reinforced by micellization/aggregation within the polymer network, hydrophobic interactions also contribute and provide a motive for excess binding.[53] On the contrary, even if hydrophobic end-tagging of peptides in the present investigation induces some amphiphilicity, no indications of peptide self-assembly were detected for these peptides in solution[36] or when incorporated into microgels (Table 2 and Figure S2 of the Supporting Information), because the fluorescence spectra clearly indicate that the environment around the indole chains is polar, also in the microgel−peptide complex.[50] This, in turn, indicates that any self-assembly of the end-tagged peptides is characterized by low aggregation numbers or close presence of the indole group to poly(acrylic acid) charges, or both.

To obtain more detailed insight into the mechanisms at play, the deswelling curves in Figure 1b where analyzed theoretically with the model described above. The theoretical curves (Figure 6 a−c) were calculated using the full model taking into account the diffusion barrier in the shell and in the "stagnant layer" in the liquid surrounding the gel. With the parameters specified above, all taken from other sources or representing equilibrium properties of the systems, the result for GKH17 and GKH17W3 is insensitive to the input value of D_{shell}, even for values as low as 10^{-15} m^2/s. This clearly shows that the rate-limiting step of the kinetics is the diffusion of peptides through the unstirred layer surrounding the microgel particle, that is, microgel deswelling kinetics is stagnant-layer-controlled.

In the calculations, C_2^* was set to 0.5 μM, but the result is largely independent also of this choice for values up to about 1 μM (recall that $C_{bulk} = 5\ \mu$M). In fact, the same result is obtained using eq 14 with $C_2^* = 0$. Although the time needed to reach the fully collapsed state does not depend on the swelling model employed in the calculations, the parameter α in eq 16 does affect the shape of the swelling curves. However, to avoid parameter fitting we used either the "nonresponsive" ($\alpha = 0$) or "responsive" ($\alpha = 1$) core model. GKH17 was found to conform best to the former, and GKH17W3 (and GKH17W6), to the latter.

The deswelling is always expected to be controlled by stagnant layer diffusion at sufficiently short times when the shell thickness is very small. This is, indeed, demonstrated from the ability of a simple stagnant layer diffusion model to capture essentially the complete deswelling curves for GKH17 and GKH17W3. The same holds for GKH17W6 at initial stages of the deswelling process (Figure 6c, dashed curve). However, for this peptide (as opposed to that of GKH17 and GKH17W3), the decay at long times is markedly influenced by intraparticle diffusion. Unfortunately, υ_{shell} is not available for this peptide (see above). However, from the condition that the experimentally observed decay rate cannot be faster than that predicted by stagnant layer control, we obtain $\upsilon_{shell} < 8 \times 10^{-4}$ m^3/mol. With this constraint, the model can be fitted reasonably well to the experimental data, but only if $D_{shell} < 10^{-16}$ m^2/s (solid line). Since values of this magnitude are small, even for reptation of

long polymer chains, it is likely that the deswelling is also influenced by other interactions, leading to slow relaxation of the shell structure. Irrespective of these concerns, however, it is clear that the deswelling kinetics for all peptides is largely controlled by stagnant layer diffusion. This is explained by the low concentration of peptide in the bulk and by the shells' being very thin (<0.5 μm), for a major part of the deswelling process, as compared to the stagnant layer thickness ($\sim$5 μm). However, for GKH17W6, the shell formed represents an additional diffusion barrier at longer times. The same is expected to apply to the KNK10 peptides because they display very similar deswelling curves (Figure 1a).

Conclusions

The interplay between electrostatic and hydrophobic interactions in microgel−peptide systems was investigated by tagging antimicrobial peptide GKH17 and its truncated version KNK10 with tryptophan oligomers of varying length. Peptide binding of these positively charged peptides to oppositely charged microgels increased with the number of tryptophan residues in the hydrophobic end tag. Peptide-induced microgel deswelling is largely controlled by stagnant layer diffusion, although for sufficiently long hydrophobic tags, the peptide−gel complexes formed in the microgel surface induce an additional barrier, reducing the deswelling kinetics. By reducing peptide−microgel electrostatic interactions through addition of salt, peptides lacking the tryptophan end tags were substantially released, whereas the end-tagged peptides remained bound to the microgels. Overall, results obtained in this study emphasize a delicate balance of electrostatic and hydrophobic interactions occurring in oppositely charged microgel−peptide systems.

Acknowledgment. This work was financed by the Swedish Foundation for Strategic Research, the Swedish Research Council (Project 621-2003-4022), and Dermagen AB. Dr. Lovisa Ringstad is acknowledged for valuable discussions.

Supporting Information Available: Titration curve of poly(acrylic acid) microgels, tryptophan fluorescence spectra for GKH17W6 in solution and when incorporated in poly(acrylic acid) microgels. This information is available free of charge via the Internet at http://pubs.acs.org.

References and Notes

(1) Eichenbaum, G. M.; Kiser, P. F.; Dobrynin, A. V.; Simon, S. A.; Needham, D. *Macromolecules* **1999**, *32*, 4867.
(2) Kamei, N.; Morishita, M.; Chiba, H.; Kavimandan, N. J.; Peppas, N. A.; Takayama, K. *J. Controlled Release* **2009**, *134*, 98.
(3) Li, Y.; de Vries, R.; Slaghek, T.; Timmermans, J.; Cohen Stuart, M. A.; Norde, W. *Biomacromolecules* **2009**, *10*, 1931.
(4) Morishita, M.; Goto, T.; Nakamura, K.; Lowman, A. M.; Takayama, K.; Peppas, N. A. *J. Controlled Release* **2006**, *110*, 587.
(5) Nolan, C. M.; Gelbaum, L. T.; Lyon, L. A. *Biomacromolecules* **2006**, *7*, 2918.
(6) Hoare, T.; Pelton, R. *Biomacromolecules* **2008**, *9*, 733.
(7) Betancourt, T.; Pardo, J.; Soo, K.; Peppas, N. A. *J. Biomed. Mater. Res., Part A* **2009**, Published online: June 17 2009, doi: 10.1002/jbm.a.32510.
(8) Bysell, H.; Hansson, P.; Malmsten, M. *J. Colloid Interface Sci.* **2008**, *323*, 60.
(9) Bysell, H.; Malmsten, M. *Langmuir* **2006**, *22*, 5476.
(10) Bysell, H.; Malmsten, M. *Langmuir* **2009**, *25*, 522.
(11) Bysell, H.; Schmidtchen, A.; Malmsten, M. *Biomacromolecules* **2009**, *10*, 2162.
(12) Johansson, C.; Hansson, P.; Malmsten, M. *J. Colloid Interface Sci.* **2007**, *316*, 350.
(13) Johansson, C.; Hansson, P.; Malmsten, M. *J. Phys. Chem. B* **2009**, *113*, 6183.
(14) Zasloff, M. *Nature* **2002**, *415*, 389.
(15) Shafer, W. *Antimicrobial Peptides and Human Disease*; Springer-Verlag: Berlin, Heidelberg, 2006.
(16) Brogden, K. A. Antimicrobial peptides: pore formers or metabolic inhibitors in bacteria? *Nat. Rev. Microbiol.* **2005**, *3*, 238.
(17) Yount, N. Y.; Bayer, A. S.; Xiong, Y. Q.; Yeaman, M. R. *Pept. Sci.* **2006**, *84*, 435.
(18) Ringstad, L.; Andersson Nordahl, E.; Schmidtchen, A.; Malmsten, M. *Biophys. J.* **2007**, *92*, 87.
(19) Ringstad, L.; Kacprzyk, L.; Schmidtchen, A.; Malmsten, M. *Biochim. Biophys. Acta, Biomembr.* **2007**, *1768*, 715.
(20) Ringstad, L.; Protopapa, E.; Lindholm-Sethson, B.; Schmidtchen, A.; Nelson, A.; Malmsten, M. *Langmuir* **2008**, *24*, 208.
(21) Ringstad, L.; Schmidtchen, A.; Malmsten, M. *Langmuir* **2006**, *22*, 5042.
(22) Nizet, V. *Curr. Issues Mol. Biol.* **2006**, *8*, 11.
(23) Jenssen, H.; Lejon, T.; Hilpert, K.; Fjell, C. D.; Cherkasov, A.; Hancock, R. E. *Chem. Biol. Drug Des.* **2007**, *70*, 134.
(24) Pasupuleti, M.; Walse, B. r.; Svensson, B.; Malmsten, M.; Schmidtchen, A. *Biochemistry* **2008**, *47*, 9057.
(25) Malmsten, M.; Davoudi, M.; Walse, B.; Rydengård, V.; Pasupuleti, M.; Mörgelin, M.; Schmidtchen, A. *Growth Factors* **2007**, *25*, 60.
(26) Nordahl, E.; Rydengård, V.; Mörgelin, M.; Schmidtchen, A. *J. Biol. Chem.* **2005**, *280*, 34832.
(27) Nordahl, E.; Rydengård, V.; Nyberg, P.; Nitsche, D.; Mörgelin, M.; Malmsten, M.; Björck, L.; Schmidtchen, A. *Proc. Natl. Acad. Sci. U.S.A.* **2004**, *101*, 16879.
(28) Pasupuleti, M.; Walse, B.; Nordahl, E. A.; Mörgelin, M.; Malmsten, M.; Schmidtchen, A. *J. Biol. Chem.* **2007**, *282*, 2520.
(29) Strömstedt, A. A.; Pasupuleti, M.; Schmidtchen, A.; Malmsten, M. *Antimicrob. Agents Chemother.* **2009**, *53*, 593.
(30) Etienne, O.; Gasnier, C.; Taddei, C.; Voegel, J.-C.; Aunis, D.; Schaaf, P.; Metz-Boutigue, M.-H.; Bolcato-Bellemin, A.-L.; Egles, C. *Biomaterials* **2005**, *26*, 6704.
(31) Etienne, O.; Picart, C.; Taddei, C.; Haikel, Y.; Dimarcq, J. L.; Schaaf, P.; Voegel, J. C.; Ogier, J. A.; Egles, C. *Antimicrob. Agents Chemother.* **2004**, *48*, 3662.
(32) Zhang, L.; Liu, Y.; Wu, Z.; Chen, H. *Drug Dev. Ind. Pharm.* **2009**, *35*, 369.
(33) Schmidtchen, A.; Frick, I.-M.; Andersson, E.; Tapper, H.; Björck, L. *Mol. Microbiol.* **2002**, *46*, 157.
(34) Silvestre, J. F.; Betlloch, M. I. *Int. J. Dermatol.* **1999**, *38*, 419.
(35) Pasupuleti, M.; Schmidtchen, A.; Chalupka, A.; Ringstad, L.; Malmsten, M. *PLoS ONE* **2009**, *4*, e5285.
(36) Schmidtchen, A.; Pasupuleti, M.; Morgelin, M.; Davoudi, M.; Alenfall, J.; Chalupka, A.; Malmsten, M. *J. Biol. Chem.* **2009**, *284*, 17584.
(37) Smith, P. K.; Krohn, R. I.; Hermanson, G. T.; Mallia, A. K.; Gartner, F. H.; Provenzano, M. D.; Fujimoto, E. K.; Goeke, N. M.; Olson, B. J.; Klenk, D. C. *Anal. Biochem.* **1985**, *150*, 76.
(38) Hoare, T.; Pelton, R. *Langmuir* **2008**, *24*, 1005.
(39) Eisenberg, D.; Schwarz, E.; Komaromy, M.; Wall, R. *J. Mol. Biol.* **1984**, *179*, 125.
(40) Hopp, T.; Woods, K. *Mol. Immunol.* **1983**, *20*, 483.
(41) Kyte, J.; Doolittle, R. F. *J. Mol. Biol.* **1982**, *157*, 105.
(42) Kiefer, J. J.; Somasundaran, P.; Ananthapadmanabhan, K. P. *Langmuir* **1993**, *9*, 1187.
(43) Kogej, K.; Theunissen, E.; Reynaers, H. *Langmuir* **2002**, *18*, 8799.
(44) Schillen, K.; Anghel, D. F.; da Graca Miguel, M.; Lindman, B. *Langmuir* **2000**, *16*, 10528.
(45) Philippova, O. E.; Hourdet, D.; Audebert, R.; Khokhlov, A. R. *Macromolecules* **1996**, *29*, 2822.
(46) Wang, C.; Tam, K. C.; Tan, C. B. *Langmuir* **2004**, *20*, 7933.
(47) Göransson, A.; Hansson, P. *J. Phys. Chem. B* **2003**, *107*, 9203.
(48) Hansson, P. *Curr. Opin. Colloid Interface Sci.* **2006**, *11*, 351.
(49) Nilsson, P.; Hansson, P. *J. Phys. Chem. B* **2007**, *111*, 9770.
(50) Strömstedt, A. A.; Pasupuleti, M.; Schmidtchen, A.; Malmsten, M. *Biochim. Biophys. Acta, Biomembr.* **2009**, *1788*, 1916.
(51) Nilsson, P.; Hansson, P. *J. Phys. Chem. B* **2005**, *109*, 23843.
(52) Coulson, J. M.; Richardson, J. F.; Blackhurst, J. R.; Harker, J. H. *Coulson & Richardson's Chemical Engineering*; Butterworth-Heinemann: Oxford, 1996.
(53) Hansson, P. *J. Phys. Chem. B* **2009**, *113*, 12903.
(54) Hansson, P.; Schneider, S.; Lindman, B. *J. Phys. Chem. B* **2002**, *106*, 9777.
(55) Nilsson, P.; Hansson, P. *J. Colloid Interface Sci.* **2008**, *325*, 316.
(56) Kyte, J.; Doolittle, R. F. *J. Mol. Biol.* **1982**, *157*, 105.

JP910068T